Environmental and Sustainability Indicators 29 (2026) 101069

Contents lists available at ScienceDirect

Environmental and Sustainability Indicators

journal homepage: www.sciencedirect.com/journal/environmental-and-sustainability-indicators

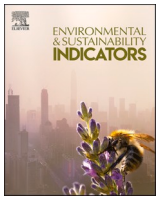

Future redistribution of *Hovenia acerba* Lindl. in China under climate change

Yangzhou Xiang [a], Suhang Li [a], Qiong Yang [a], Ying Liu [b], Jiaojiao Liu [a], Bin Yao [c,*], Yuan Li [d,**]

[a] School of Geography and Resources, Guizhou Education University, Guiyang, 550018, China
[b] School of Biological Sciences, Guizhou Education University, Guiyang, 550018, China
[c] State Key Laboratory of Tree Genetics and Breeding, Institute of Ecology Conservation and Restoration, Chinese Academy of Forestry, Beijing, 100091, China
[d] Grasslands and Sustainable Farming, Production Systems unit, Natural Resources Institute Finland (Luke), Halolantie 31A, Maaninka, FI−71750, Finland

ARTICLE INFO

Keywords:
Hovenia acerba Lindl.
Climate change
MaxEnt model
Species distribution prediction
Suitable habitat

ABSTRACT

Hovenia acerba Lindl. is valued for its medicinal properties and role in maintaining ecosystem integrity, particularly through soil stabilization. However, climate change poses significant challenges to its natural distribution. This study employed an optimized Maximum Entropy (MaxEnt) model alongside BCC-CSM2-MR climate projections to predict the impacts of climate change on the distribution of *H. acerba* in China and to identify key environmental determinants. We found that precipitation in the driest month (Bio14) and minimum temperature of the coldest month (Bio6) are the primary factors governing its distribution. Under current climatic conditions, the potential suitable habitat for *H. acerba* covers approximately 29.15 % of China's land area. Future projections indicate a consistent expansion of suitable habitats under all climate scenarios, with a notable northwestward shift in the distribution centroid from Hunan to Hubei Province. These findings highlight the resilience of *H. acerba* to climate change and provide critical insights for its conservation and sustainable management under future climatic conditions.

1. Introduction

Climate change represents one of the most significant challenges to global biodiversity, with profound implications for species distribution patterns and ecosystem dynamics. Rising temperatures, altered precipitation regimes, and increased frequency of extreme weather events have already begun to reshape the geographical ranges of numerous plant species (Dolezal et al., 2021; Wang et al., 2024). Understanding these distribution shifts is crucial for developing effective conservation strategies and sustainable resource management approaches, particularly for species with significant ecological and economic value. A prime example of such a species is *Hovenia acerba* Lindl., whose ecological functions and economic benefits make it an ideal model for studying climate change impacts.

H. acerba, a deciduous tree species in the *Rhamnaceae* family, holds substantial importance in traditional Chinese medicine, erosion control, and ecological protection. The species produces fruits and leaves rich in bioactive compounds, including flavonoids, saponins, and polysaccharides, which have demonstrated efficacy in treating various ailments such as hepatitis and hyperglycemia (Kong et al., 2023; Ma and Zhou, 2022). The hepatoprotective properties of its seeds and potential anti-diabetic effects of its leaves have been extensively documented in pharmacological studies (Ma and Zhou, 2022). Beyond its medicinal applications, the wood of *H. acerba* is valued for its durability in furniture making and construction, contributing to its economic significance.

Ecologically, *H. acerba* contributes significantly to slope stabilization and erosion mitigation. Its extensive root system enhances soil structure and water infiltration, making it a key species for rehabilitating degraded landscapes (Ding et al., 2009; Zhang, 2015). This characteristic has positioned *H. acerba* as a key species in reforestation and afforestation initiatives targeting degraded landscapes. Additionally, the species contributes to biodiversity maintenance by providing habitat and food resources for various fauna, thereby supporting complex ecological networks (Teng and Zhou, 2016; Yu et al., 2008).

Climate change is triggering a fundamental restructuring of global species distributions, challenging plant survival and ecological fitness. As key regulators of physiological processes, reproduction, and species interactions, climatic variables—especially temperature and

* Corresponding author.
** Corresponding author.
E-mail addresses: acmn21@caf.ac.cn (B. Yao), yuan.li@luke.fi (Y. Li).

https://doi.org/10.1016/j.indic.2025.101069
Received 13 April 2025; Received in revised form 11 November 2025; Accepted 1 December 2025
Available online 2 December 2025

precipitation—drive complex ecological responses (An et al., 2020; Gong et al., 2020). Rising temperatures force species to shift along altitudinal and latitudinal gradients (Lindborg et al., 2021; MacDougall et al., 2021), while changing precipitation patterns impair phenology and reproductive success (Ganjurjav et al., 2020; Numata et al., 2022). Such climate-induced changes ultimately reshape plant communities, ecosystem functions, and associated services. To quantify these effects, species distribution models (SDMs) have become essential tools. The Maximum Entropy (MaxEnt) approach excels particularly with presence-only data, producing reliable projections (Elith et al., 2011; Zhao et al., 2022). Its applications demonstrate considerable value: MaxEnt has revealed range losses in *Pinus gerardiana* across South Asia (Khan et al., 2022) and predicted extensive expansion of *Broussonetia papyrifera* in China (Wang and Guan, 2023). These examples confirm that combining mechanistic models with climate scenarios offers a robust framework for anticipating how species respond to environmental transformation.

While existing studies have extensively documented the germplasm resources, phytochemical composition, and pharmacological properties of *H. acerba* (Cheng et al., 2023; Peng et al., 2018; Yang et al., 2023; Yu et al., 2020; Zhang et al., 2023), a critical knowledge gap remains regarding how climate change will affect its geographical distribution. Most existing studies lack a robust, climate-scenario-driven projection, and none have employed an optimized species distribution modeling framework to address this question for *H. acerba*. To bridge this gap, our study introduces a novel approach by integrating a rigorously optimized MaxEnt model with the latest BCC-CSM2-MR climate projections from CMIP6. This methodology not only enhances the predictive accuracy for *H. acerba* but also provides a refined framework for assessing climate change impacts on economically important tree species. The findings are crucial for developing science-based conservation strategies.

This study aims to comprehensively assess the potential impacts of climate change on the distribution of *H. acerba* in China by integrating an optimized MaxEnt model with climate projections from the BCC-CSM2-MR model. Our specific objectives are: (1) To identify the key environmental factors governing the current distribution of *H. acerba*. (2) To predict potential shifts in its suitable habitat under multiple climate change scenarios (SSP1-2.6, SSP2-4.5, and SSP5-8.5) for the 2050s, 2070s, and 2090s. (3) To quantify directional changes in the species' distribution centroid to elucidate its spatial migration trajectory. We hypothesized that warming temperatures would drive northward and upward shifts in suitable habitat, with expansion rates varying significantly across emissions scenarios. The findings from this research would provide a scientific foundation for developing targeted conservation interventions and adaptive management strategies for *H. acerba* under changing climatic conditions.

2. Materials and methods

2.1. Collecting occurrence data of H. acerba

Species occurrence records were compiled from multiple biodiversity databases, including the Global Biodiversity Information Facility (https://www.gbif.org), the Chinese Virtual Herbarium (http://www.cvh.org.cn), the National Specimen Information Infrastructure of China (http://www.nsii.org.cn), Google Scholar (https://scholar.google.com), and the China National Knowledge Infrastructure (https://book.oversea.cnki.net). This comprehensive search yielded 1206 initial distribution records of *H. acerba* within China. For records lacking direct coordinate information, precise textual locations were georeferenced using an online coordinate picking system. All coordinates were then visually verified against high-resolution basemaps in ArcGIS, with implausible records (e.g., in oceans or ambiguous areas) being removed. To mitigate spatial sampling bias and model overfitting, a spatial rarefaction was applied by retaining only one record per 2.5 × 2.5′ grid cell, resulting in 1024 unique records for subsequent analysis

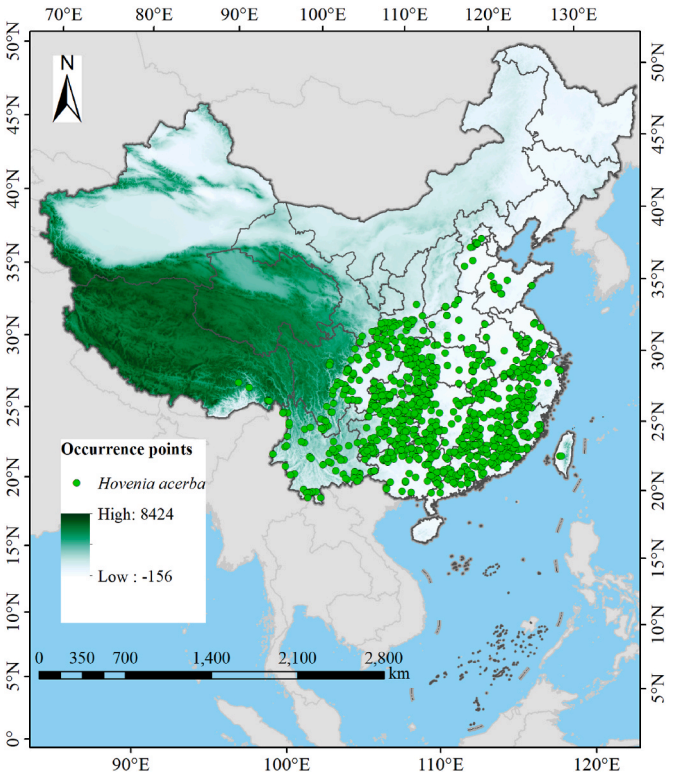

Fig. 1. Current geographic distribution and distribution points of *H. acerba* in China.

(Fig. 1). The filtered coordinates were subsequently exported to a CSV file for subsequent modeling. Additionally, the map depicting China's administrative divisions (map approval designation GS (2023)2762) was obtained from the Standard Map Service online platform (http://bzdt.ch.mnr.gov.cn).

2.2. Environmental variables

Nineteen climatic factors (bio1-bio19) from the WorldClim version 2.1 climate data for current (1970–2000) and future climate scenarios (https://www.worldclim.org) were selected as environmental factors (Table 1). The future climate data is selected for three periods: the 2050s

Table 1
Environmental variables used in this study.

Variables	Description	Units	Contribution rate (%)
Bio1	Annual mean temperature	°C	0.3
Bio2	Mean diurnal range(Mean of monthly)	°C	1.4
Bio3	Isothermality (Bio2/Bio7) (× 100)		0.8
Bio4	Standard deviation of temperature seasonality		2.0
Bio5	Max temperature of warmest month	°C	1.5
Bio6	Min temperature of coldest month	°C	22.8
Bio7	Temperature annual range (Bio5-Bio6)	°C	1.5
Bio8	Mean temperature of wettest quarter	°C	1.3
Bio9	Mean temperature of driest quarter	°C	0.2
Bio10	Mean temperature of warmest quarter	°C	0.6
Bio11	Mean temperature of coldest quarter	°C	0.4
Bio12	Annual precipitation	mm	31.3
Bio13	Precipitation of wettest month	mm	0.2
Bio14	Precipitation of driest month	mm	32.5
Bio15	Variation of precipitation seasonality		1.8
Bio16	Precipitation of wettest quarter	mm	0.3
Bio17	Precipitation of driest quarter	mm	0.4
Bio18	Precipitation of warmest quarter	mm	0.2
Bio19	Precipitation of coldest quarter	mm	0.5

(2041–2060), the 2070s (2061–2070), and the 2090s (2081–2100). We employed three Shared Socioeconomic Pathways scenarios within the Sixth Coupled Model Intercomparison Project (CMIP6), specifically under the BCC-CSM2-MR model (Zhou et al., 2020), which has shown good predictive performance over China.

In addition, three Representative Concentration Pathways are selected to assess the distribution of suitable habitat of *H. acerba* in the future: SSP1-2.6, SSP2-4.5 and SSP5-8.5, each corresponding to scenarios of minimal, moderate, and substantial greenhouse gas emissions, respectively (Zhao et al., 2024). To enhance model accuracy by reducing redundancy among environmental factors (Mendes et al., 2020), we employed a two-step variable selection process to mitigate multicollinearity. This involved calculating pairwise correlation coefficients for all 19 bioclimatic variables and eliminating one variable from any pair with $|r| > 0.75$, prioritizing the removal of the variable with the lower contribution rate (Zhang et al., 2018). This widely adopted threshold effectively controls multicollinearity while preserving a sufficient set of ecologically meaningful predictors. The final selection also considered the contribution magnitude of each variable from the MaxEnt model (Table 1; Fig. 2), resulting in eight key variables for final modeling.

Ultimately, eight environmental factors were selected for model building, specifically Bio2 (Mean diurnal range (Mean of monthly)), Bio4 (Standard deviation of temperature seasonality), Bio5 (Max temperature of the warmest month), Bio6 (Min temperature of the coldest month), Bio8 (Mean temperature of the wettest quarter), Bio14 (Precipitation of the driest month), Bio15 (Variation of precipitation seasonality), Bio16 (Precipitation of the wettest quarter).

2.3. MaxEnt model optimization and modeling

2.3.1. Optimization of MaxEnt model

To precisely forecast the probable distribution range of *H. acerba*, we employed the R package 'ENMeval' to optimize the MaxEnt model by modifying two key constraint parameters: the Regularization Multiplier (RM) and the Feature Combination (FC) (Warren and Seifert, 2011). We randomly divided the 1024 distribution records into a training set (75 %) and a testing set (25 %) to assess the model's generalization ability. To investigate the model's performance under various levels of regularization strength, The MaxEnt model was optimized using the R package ENMeval to identify the optimal combination of regularization multiplier (RM) and feature class (FC). This optimization is critical to prevent overfitting and to improve model transferability to future climate scenarios. The best model was selected based on the lowest Akaike Information Criterion corrected (AICc), which balances model complexity and goodness-of-fit. While employing both the 10 % Training Omission Rate (OR10) and the discrepancy in the Area Under the Curve (AUC) between training and testing (AUC.DIFF) to mitigate the risk of model overfitting (Shi et al., 2024). After a comprehensive assessment, we constructed the final model using the optimized regularization multiplier and feature combination corresponding to a delta AICc of zero.

2.3.2. MaxEnt modeling

The geographical coordinates of 1024 distribution points along with eight bioclimate variables were imported into the Maxent software (Version 3.4.1) (Steven J. Phillips et al.). Randomly select 75 % of the *H. acerba* sample distribution point data for simulation training, with the remaining 25 % of the data serving as the test training set. The optimized RM and FC parameters are chosen, and the model is run 10 times, selecting the Logistic mode as the output type. The area under the curve (AUC) of the receiver operating characteristics curve (ROC) is used to verify the simulation effectiveness of the model (Li et al., 2020). The model's training data, as evaluated by the ROC curve, had an average AUC value of 0.878 with a standard deviation of 0.009 across 10 replicate runs. This high AUC value coupled with a low standard deviation indicates consistently excellent and reliable predictive performance. Furthermore, we complemented the AUC evaluation with the examination of the omission rate and AICc during model optimization to guard against overfitting, ensuring that the model's robustness was not solely dependent on a single metric.

2.4. Classification of potentially suitable areas of H. acerba

The average values from the 10 repetitions processed by the Maxent model are taken as the basic data for the division of the suitable living area for the *H. acerba*. The output results are converted into TIF format raster data using the format conversion function in ArcGIS 10.8. The potential suitable habitat areas for *H. acerba* are divided according to the natural break method, combined with the distribution patterns of the species, into unsuitable areas (0–0.1), generally suitable areas (0.1–0.3),

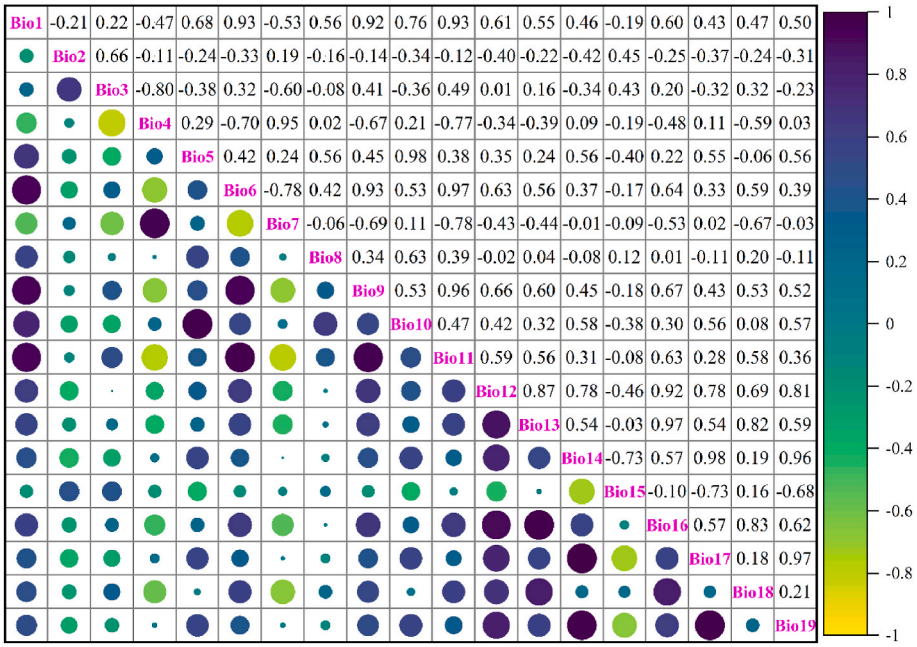

Fig. 2. Correlation analysis of environmental factors.

moderately suitable areas (0.3–0.5), and highly suitable areas (0.5–1) (Zhang et al., 2024). The raster processing capabilities of the ArcGIS software were utilized to perform area calculations on the reclassified layers, thereby determining the proportion of each area. Subsequently, based on the actual area of the national territory, these proportions were converted into specific area for each grade (Zhang et al., 2022).

2.5. Analysis of the spatial pattern changes in the suitable habitat area for *H. acerba*

Under the impact of climate change, the spatial pattern of species' suitable habitats can be divided into three situations: stability areas, contraction areas, and expansion areas (LÜ et al., 2024). Based on the predicted suitable habitat results for *H. acerba* across different periods, we categorized areas with a logical value ≥ 10 % as suitable habitats, which include low, medium, and high suitability zones. Areas with a logical value < 10 % were deemed non-suitable. Using these classifications, we constructed a presence/absence (1, 0) matrix to compare the past with the present, and the present with future climate environments. The changes in area between the past and the future are both compared and calculated based on the current potential suitable habitat area of *H. acerba*, with the matrix value $0 \rightarrow 1$ representing the gain area, $1 \rightarrow 0$ representing the loss area, and $1 \rightarrow 1$ representing the stable area (Ye et al., 2020). Finally, the matrix values are transformed into attribute values and imported into the ArcGIS 10.8 software to create a map showing the changes in the spatial pattern of *H. acerba*'s suitable habitats.

2.6. Core distributional shifts under different climatic scenarios

The probability results of the suitable distribution areas for *H. acerba* obtained from the model calculations are reclassified, that is, spatial units with a species existence probability value ≥ 0.1 are defined as suitable habitats for *H. acerba*, and spatial units with a species distribution probability value < 0.1 are defined as unsuitable areas (Zhang et al., 2019). The geometric centroid of the spatial units with a species distribution probability value ≥ 0.1 is defined as the distribution center point of the suitable habitat for *H. acerba*. The location of the distribution center point represents the overall spatial position of the species' suitable habitat, and the migration trend and distance of the distribution center point are used to characterize the overall migration trend and distance of the species' suitable habitat area.

To analyze shifts in the distribution centroid of *H. acerba*, we conducted centroid shift analysis using binary outputs with the highest AUC values from the MaxEnt model across all future periods and climate scenarios. The analysis was performed with the SDM toolbox, a Python-based GIS toolkit designed for species distribution modeling (Qian, 2022), which enables comparative analysis of current and future habitat centroids. This approach allows quantification of how climate change influences species distributions through geometric center displacements (Huan et al., 2023). Specifically, we employed the Centroid Changes tool within the SDMToolbox (Brown et al., 2017) to project future distribution centroids and assess climate change impacts across different periods and SSP scenarios. To quantify the directional shift of the species' suitable habitat, the distribution centroid was calculated for each scenario using the SDM toolbox.

3. Results

3.1. Model optimization and accuracy evaluation

The parameter tuning of the MaxEnt model by ENMeval revealed that at RM = 1.0 and FC = LQHPT, the model achieved the lowest AICc score, with an AICc value reaching zero (Fig. 3a). A subsequent analysis showed that this model's AUC.DIFF was elevated by 37.92 % in comparison to the model with default settings (RM = 1.0 and FC = LQHP) (Fig. 3b). Moreover, the OR10 value for this model was reduced by 20.04 % compared to the default model (Fig. 3c). Consequently, the parameters RM = 1.0 and FC = LQHPT were selected as the optimal configuration. The model's training data, as evaluated by the ROC curve, had an average AUC value of 0.878 with a standard deviation of

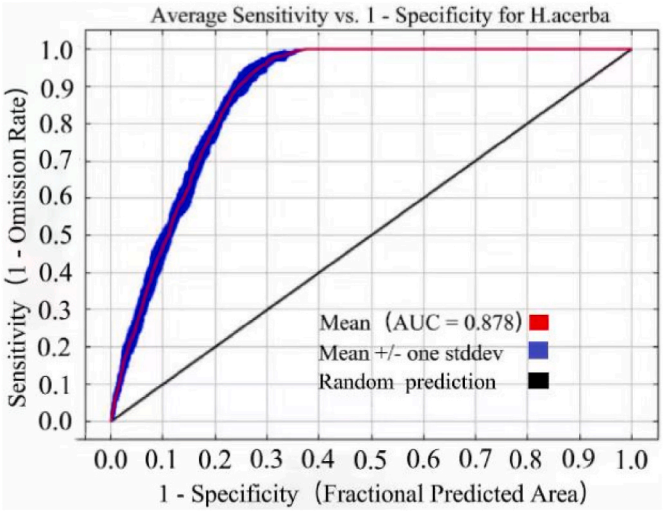

Fig. 4. Receiver operator characteristic (ROC) curve tests the accuracy of MaxEnt model.

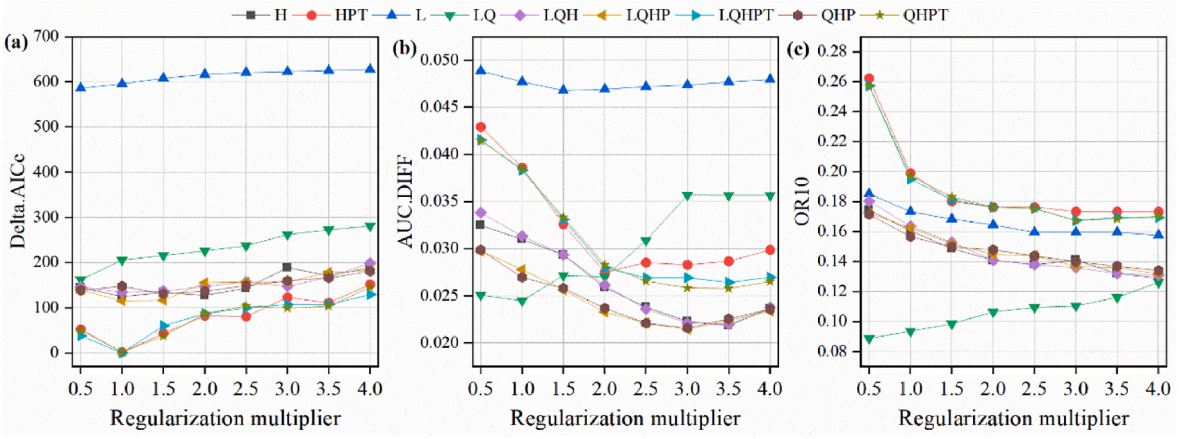

Fig. 3. Delta.AICc (a), AUC.DIFF (b), and OR10 (c) of models with different parameter combinations resulted from MaxEnt models.

0.009 (Fig. 4), demonstrating the model's robust predictive capability.

3.2. Analysis of critical environmental variables

Two environmental variables, namely both Precipitation of driest month (Bio14) and Min temperature of coldest month (Bio6) contributed 87.4 % to the model's predictive power. Precipitation of driest month (Bio14) alone explained 55.5 % of the total variance and was identified as the primary factor influencing the spatial distribution of *H. acerba* (Fig. 5a). To deepen the understanding of the relationship between key factors and the likelihood of *H. acerba* growth, this study has plotted the response curves of the dominant factors when relying solely on individual environmental variables. Using a logistic output threshold of 0.1 to differentiate suitable and unsuitable growth areas for *H. acerba*, the suitable precipitation range for its growth is 0–190 mm (Fig. 5b), and the minimum temperature range is −14.6–16.8 °C (Fig. 5c). The suitable precipitation range indicates that *H. acerba* can tolerate a wide range of precipitation conditions, from relatively dry to quite wet. This wide range of suitable precipitation suggests that water availability is not a limiting factor for its growth across most regions. The minimum temperature range shows that *H. acerba* can survive in areas with quite cold winters (down to −14.6 °C) as well as milder ones, up to relatively warm temperatures (16.8 °C). This indicates that *H. acerba* is adaptable to a broad range of temperature conditions, making it a resilient species that can thrive in diverse climates.

3.3. Potential distribution under current climate

Under current climatic conditions, the potential total suitable habitat area for *H. acerba* is 279.8 × 10^4 km^2, accounting for approximately 29.15 % of China's total land area (Fig. 6). The area of *H. acerba*'s moderately low suitable habitat is approximately 64.86 × 10^4 km^2, which accounts for 6.76 % of the total national land area; the moderately suitable habitat area is about 116.07 × 10^4 km^2, representing 12.09 % of the national land area; and the high suitable habitat area is approximately 98.87 × 10^4 km^2, only making up 10.30 % of the total national land area. Under current climatic conditions, the high suitable habitat areas for *H. acerba* mainly include Chongqing Municipality, Guizhou Province, Guangxi Zhuang Autonomous Region, Guangdong Province, Fujian Province, Jiangxi Province, Hunan Province, and the northeastern part of Sichuan Province; the moderately suitable habitat areas mainly include Yunnan Province, Hubei Province, Anhui Province, Zhejiang Province, Shaanxi Province, Jiangsu Province, and Taiwan Province; the low suitable habitat areas mainly include Shandong Province, Hebei Province, and Henan Province. The non-suitable habitat areas for *H. acerba* are primarily distributed in the northwest and north of China. The boundary between the suitable and non-suitable areas generally coincides with 400 mm annual precipitation line in China, along with the three northeastern provinces in China.

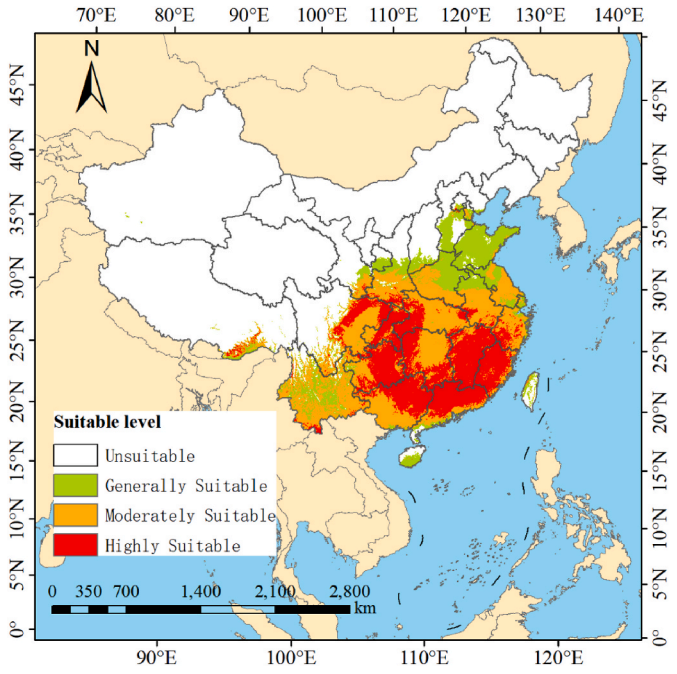

Fig. 6. Distribution of current suitable areas of *H. acerba* in China based on MaxEnt.

3.4. Suitable areas distribution of the H. acerba under future climate

Under the SSP1-2.6 climate scenario, total suitable habitat area for *H. acerba* is predicted to be 288.15 × 10^4 km^2 by the 2050s, with high, medium, and low suitable habitats covering 125.51 × 10^4 km^2, 94.58 × 10^4 km^2, and 68.05 × 10^4 km^2 respectively. High suitability areas are mainly in Chongqing, Guizhou, Fujian, Jiangxi, Hunan, Zhejiang, Hebei, Hubei, Beijing, eastern Sichuan, and northern Guangdong (Fig. 7a). By the 2070s, the total area slightly decreases to 285.54 × 10^4 km^2, with high, medium, and low suitable habitats at 93.66 × 10^4 km^2, 107.07 × 10^4 km^2, and 84.81 × 10^4 km^2 respectively, and the distribution of high suitability areas remains largely the same (Fig. 7d). By the 2090s, the total suitable habitat area increases to 289.77 × 10^4 km^2, with high, medium, and low suitable habitats at 108.85 × 10^4 km^2, 101.25 × 10^4 km^2, and 79.67 × 10^4 km^2 respectively, and the high suitability distribution like previous decades (Fig. 7g).

Under the SSP2-4.5 scenario, by the 2050s, the total suitable habitat area expands to 304.18 × 10^4 km^2, with high, medium, and low suitable habitats at 114.66 × 10^4 km^2, 102.77 × 10^4 km^2, and 86.75 × 10^4 km^2

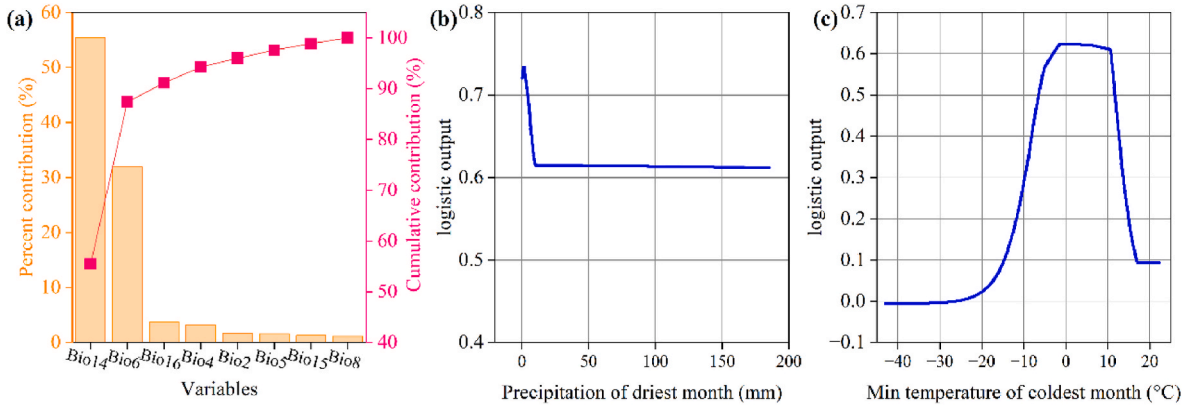

Fig. 5. Response curve of dominant environmental factors for *H. acerba*.

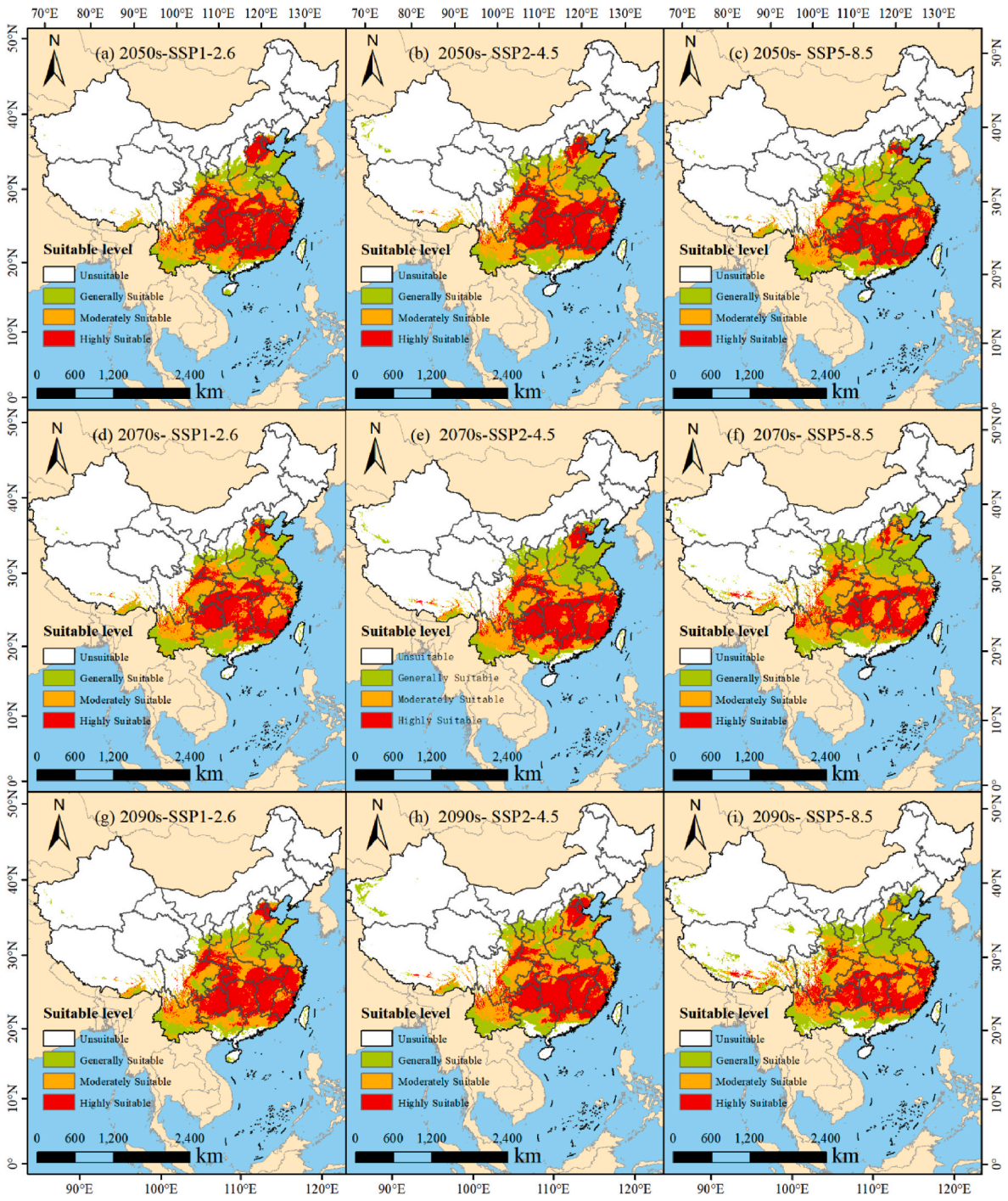

Fig. 7. Potentially suitable areas of *H. acerba* in China under future different climate scenarios in various periods.

respectively. High suitability areas are primarily in Chongqing, Guizhou, Fujian, Jiangxi, Hunan, Zhejiang, Hebei, Beijing, and eastern Sichuan (Fig. 7b). By the 2070s, the total area further increases to 309.72 $\times$ 10^4 km^2, with high, medium, and low suitable habitats at 112.37 $\times$ 10^4 km^2, 102.34 $\times$ 10^4 km^2, and 95.01 $\times$ 10^4 km^2 respectively, and high suitability areas extending to northern Guangdong (Fig. 7e). By the 2090s, the total suitable habitat area reaches 315.16 $\times$ 10^4 km^2, with high, medium, and low suitable habitats at 111.35 $\times$ 10^4 km^2, 112.03 $\times$ 10^4 km^2, and 91.78 $\times$ 10^4 km^2 respectively, and the distribution pattern continuing (Fig. 7h).

Under the SSP5-8.5 scenario, by the 2050s, total suitable habitat area is 299.48 $\times$ 10^4 km^2, with high, medium, and low suitable habitats at 95.40 $\times$ 10^4 km^2, 103.64 $\times$ 10^4 km^2, and 100.44 $\times$ 10^4 km^2 respectively. High suitability areas are mainly in Chongqing, Guizhou, Fujian, Jiangxi, Hunan, Zhejiang, Beijing, eastern Sichuan, and northern Guangdong (Fig. 7c). By the 2070s, the total area increases to 314.85 $\times$ 10^4 km^2, with high, medium, and low suitable habitats at 79.47 $\times$ 10^4 km^2, 128.20 $\times$ 10^4 km^2, and 107.18 $\times$ 10^4 km^2 respectively, and high suitability areas shifting to Guizhou, Fujian, Jiangxi, Hunan, Zhejiang, eastern Chongqing, southern Hebei, and central Sichuan (Fig. 7f). By the 2090s, the total suitable habitat area is 319.80 $\times$ 10^4 km^2, with high, medium, and low suitable habitats at 80.06 $\times$ 10^4 km^2, 116.92 $\times$ 10^4 km^2, and 122.82 $\times$ 10^4 km^2 respectively, and high suitability areas mainly in Chongqing, Guizhou, Fujian, Hunan, Zhejiang, western

Jiangxi, northern Yunnan, and central and southern Sichuan (Fig. 7i).

3.5. Dynamic change of the predicted potentially suitable area for *H. acerba*

Compared to current suitable habitat areas, those of *H. acerba* under three future climate scenarios all show expansion exceeding loss (Fig. 8). Under SSP1-2.6, by the 2050s, retained suitable habitat is 328.03 × 10^4 km^2 (89.97 % stable), lost area is 8.62 × 10^4 km^2 (2.37 % loss), and expanded area is 27.93 × 10^4 km^2 (7.66 % expansion) (Fig. 8a). By the 2070s, retained area slightly decreases to 326.29 × 10^4 km^2 (89.88 % stable), lost area increases to 10.39 × 10^4 km^2 (2.86 % loss), and expanded area decreases to 26.36 × 10^4 km^2 (7.26 % expansion) (Fig. 8d). By the 2090s, retained area further decreases to 324.62 × 10^4 km^2 (87.73 % stable), lost area increases to 12.03 × 10^4 km^2 (3.25 % loss), and expanded area rises to 33.36 × 10^4 km^2 (9.02 % expansion) (Fig. 8g).

Under SSP2-4.5, by the 2050s, retained suitable habitat is 323.79 × 10^4 km^2 (83.34 % stable), lost area is 12.86 × 10^4 km^2 (3.31 % loss), and expanded area is 51.58 × 10^4 km^2 (13.35 % expansion) (Fig. 8b). By the 2070s, retained area increases to 325.76 × 10^4 km^2 (82.81 % stable), lost area decreases to 10.90 × 10^4 km^2 (2.77 % loss), and expanded area rises to 56.73 × 10^4 km^2 (14.42 % expansion) (Fig. 8e). By the 2090s, retained area decreases to 321.38 × 10^4 km^2 (79.46 % stable), lost area

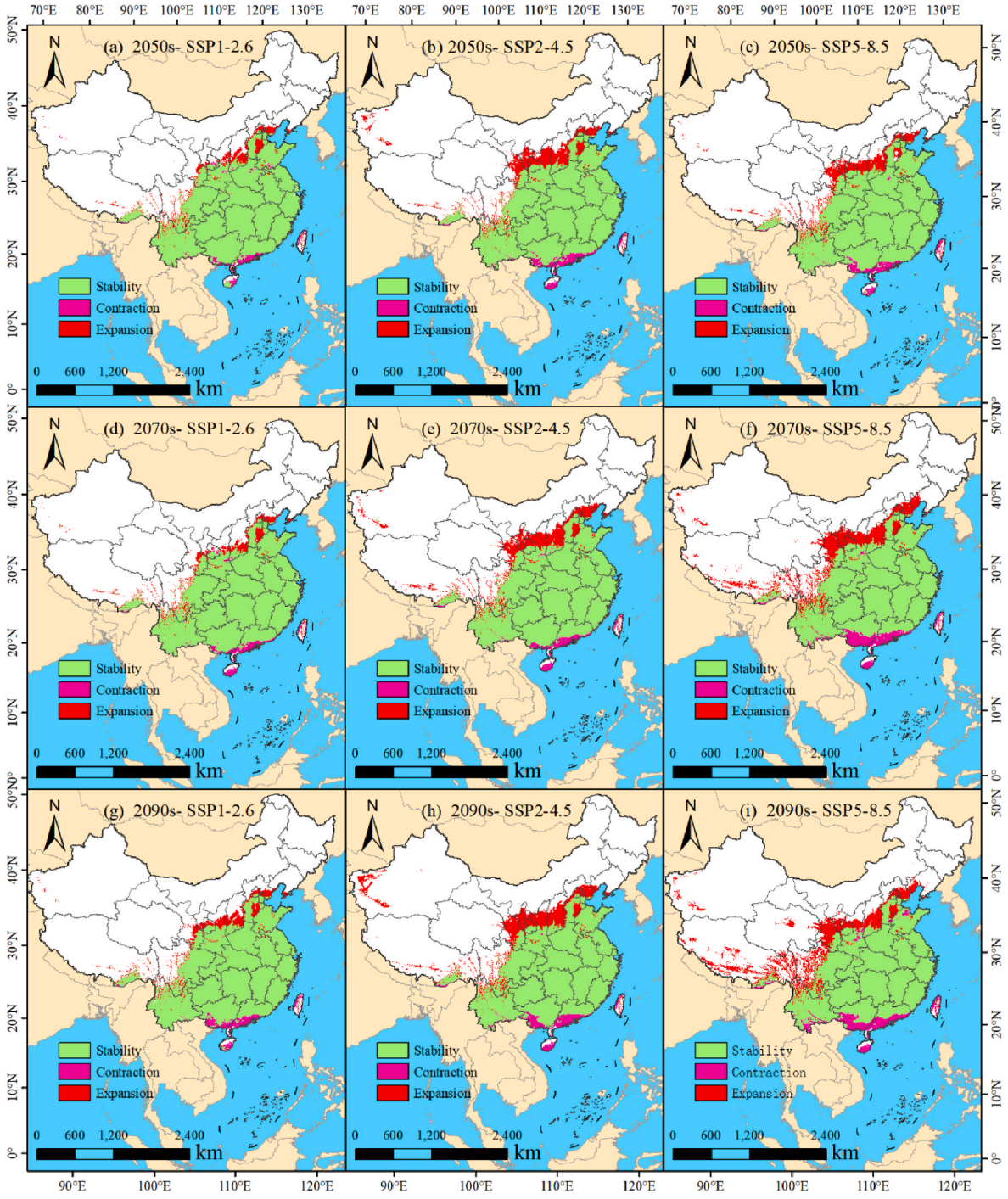

Fig. 8. Spatial transformation pattern of the predicted potentially suitable areas for *H. acerba* (compared to the current range).

increases to 15.28 × 10^4 km^2 (3.78 % loss), and expanded area further increases to 67.77 × 10^4 km^2 (16.76 % expansion) (Fig. 8h).

Under SSP5-8.5, by the 2050s, retained suitable habitat is 325.03 × 10^4 km^2 (85.22 % stable), lost area is 11.61 × 10^4 km^2 (3.04 % loss), and expanded area is 44.77 × 10^4 km^2 (11.74 % expansion) (Fig. 8c). By the 2070s, retained area decreases to 315.12 × 10^4 km^2 (76.81 % stable), lost area increases to 21.53 × 10^4 km^2 (5.25 % loss), and expanded area rises significantly to 73.61 × 10^4 km^2 (17.94 % expansion) (Fig. 8f). By the 2090s, retained area further decreases to 311.83 × 10^4 km^2 (74.30 % stable), lost area increases to 24.80 × 10^4 km^2 (5.91 % loss), and expanded area reaches 83.05 × 10^4 km^2 (19.79 % expansion) (Fig. 8i).

3.6. Migration of potential distribution centroid of *H. acerba* under different climatic scenarios

The distribution center of *H. acerba* is projected to shift northwest across future climate scenarios (Fig. 9). Currently, the centroid is in Gaojiao Town, Cili County, Zhangjiajie City, Hunan Province (110°60′E, 29°11′N). Under SSP1-2.6, by the 2050s, the centroid moves northwest to Zouma Baizu Township, Sangzhi County, Zhangjiajie City (110°50′E, 29°42′N), 59.86 km from the current location. By the 2070s, it shifts further northwest 7.36 km to Luoping Township, Shimen County, Changde City (110°47′E, 29°45′N). By the 2090s, it moves north 22.32 km to Hupingshan Town, Shimen County (110°48′E, 29°57′N). Under SSP2-4.5, by the 2050s, the centroid migrates 138.19 km northwest to Fugan Township, Wufeng Tujia Autonomous County, Yichang City, Hubei Province (110°26′E, 30°19′N). There is little change by the 2070s. By the 2090s, it moves 53.09 km northwest to Gaoping Town, Jianshi County, Enshi Autonomous Prefecture (110°01′E, 30°36′N). Under SSP5-8.5, by the 2050s, the centroid shifts 108.67 km northwest to Wufeng Town, Wufeng Tujia Autonomous County (110°36′E, 30°06′N). By the 2070s, it moves 76.17 km northwest to Gaoping Town, Jianshi County

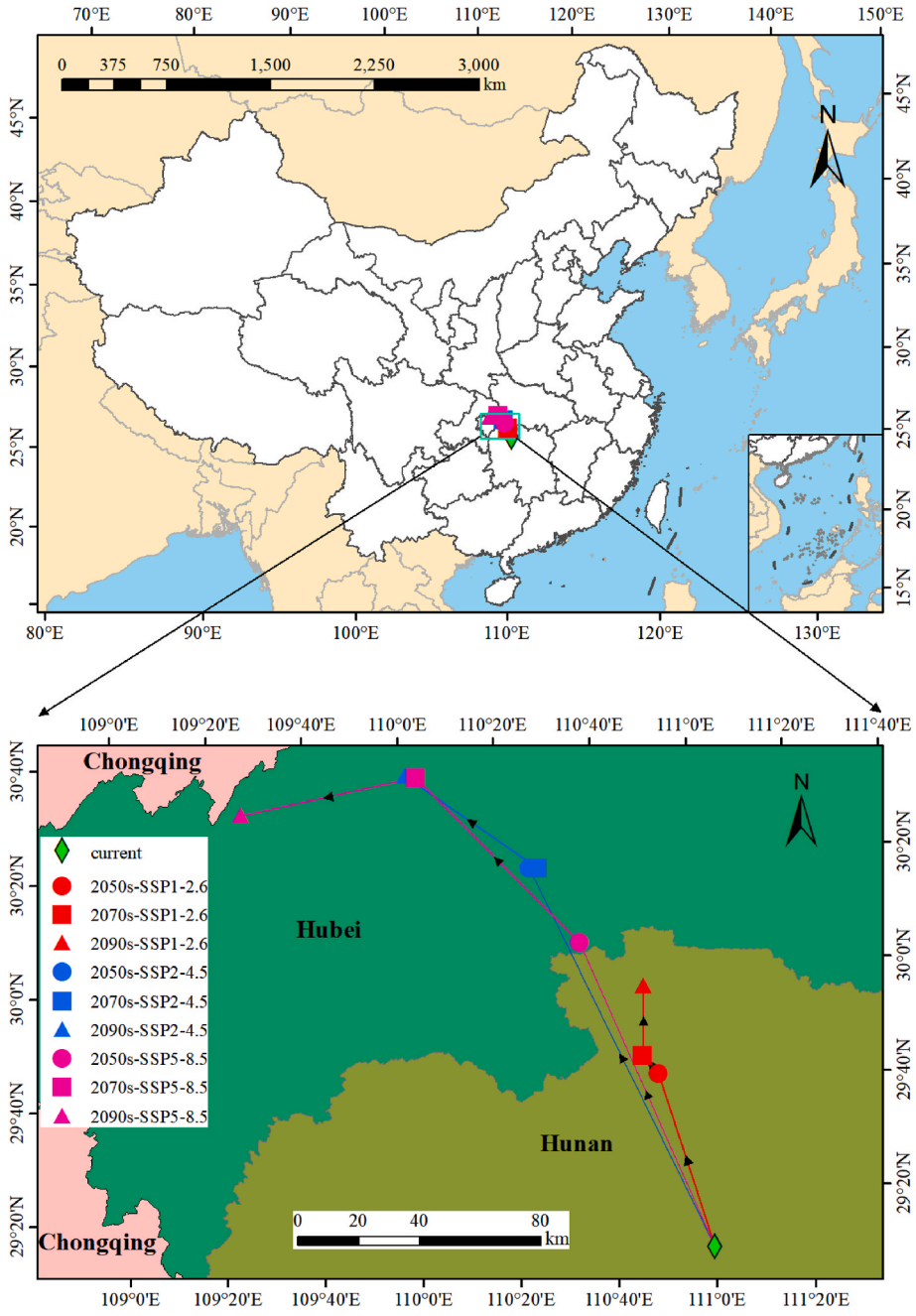

Fig. 9. Migration location of the center of suitable areas of *H. acerba* under different climate change scenarios.

(110°03′E, 30°36′N). By the 2090s, it relocates 59.26 km southwest to Taiyanghe Township, Enshi City (109°27′E, 30°31′N).

4. Discussion

4.1. MaxEnt model performance for H. acerba

The high predictive performance of our optimized MaxEnt model (AUC = 0.878 ± 0.009) underscores the reliability of our distribution projections (Elith et al., 2006). More importantly, the substantial gains in model fit after parameter tuning highlight a critical methodological insight: the application of off-the-shelf default settings can yield sub-optimal predictions for species with complex niches like *H. acerba* (Muscarella et al., 2014). The optimal model configuration (RM = 1.0, FC = LQHPT) was selected based on the lowest Akaike Information Criterion (AICc), effectively balancing model complexity and predictive power. This optimized model showed a 37.92 % increase in AUC.DIFF and a 20.04 % reduction in OR10 compared to the default settings, quantitatively confirming the mitigation of overfitting and the enhancement of model accuracy. This finding emphasizes the necessity of model optimization in ecological forecasting to generate credible results for conservation planning, a conclusion that aligns with a growing body of methodological research (Shi et al., 2024).

4.2. Critical climate factors affecting the distribution of H. acerba in China

Our identification of dry-season precipitation (Bio14) and minimum winter temperature (Bio6) as the dominant constraints on *H. acerba*'s distribution reveals its core climatic niche, a finding consistent with the climate envelope theory for subtropical tree species (Pearson and Dawson, 2003). This dual dependency suggests that the species is vulnerable to two primary climate change threats: intensified drought stress, a key driver of tree mortality in warming climates (Allen et al., 2010), and the potential disruption of cold-induced dormancy cycles due to winter warming, which can impair the fitness of temperate and subtropical trees (Chuine, 2010). The response curves defined the species' fundamental niche: suitable growth occurs when precipitation of the driest month (Bio14) is between 0 and 190 mm and the minimum temperature of the coldest month (Bio6) is between −14.6 °C and 16.8 °C (Fig. 5). These quantitative thresholds are critical for identifying areas where future climate may exceed the species' physiological tolerances, an approach central to vulnerability assessments (Williams et al., 2008). Consequently, regions projecting concurrent increases in dry-season aridity and minimum temperatures may become future climate change hotspots for population decline, underscoring the importance of identifying such geographic disparities in climate exposure (Mantyka-Pringle et al., 2015).

4.3. Potential spatiotemporal pattern of H. acerba under different climate change scenarios

Our projections reveal a consistent trend of habitat expansion for *H. acerba* across all future climate scenarios, though the magnitude and spatial configuration of these shifts are highly dependent on the emissions pathway. Under the high-emissions scenario (SSP5-8.5), the total suitable habitat is projected to expand by 19.79 % by the 2090s, the most significant increase among all scenarios. This net expansion, however, masks a concurrent and ecologically critical habitat loss of 5.91 % in current core southern regions, highlighting a complex redistribution rather than a simple range increase (Chen et al., 2011; Lenoir and Svenning, 2015; Zhu et al., 2012).

This divergent response, expansion in the northwest and contraction in parts of the south, can be attributed to the species' specific climatic niche defined by its physiological tolerances. The northwestward shift is primarily driven by the alleviation of cold limitations in previously marginal areas, allowing the species to track its suitable climate envelope (Feeley et al., 2020; Freeman et al., 2018). Conversely, habitat loss in the south is likely due to the exceedance of upper thermal tolerance limits and potential alterations in dry-season precipitation patterns, pushing conditions beyond the species' physiological optimum and increasing its vulnerability to hydraulic failure (Allen et al., 2010; Choat et al., 2012).

The projected redistribution of *H. acerba* signifies more than a geographical shift; it portends a potential reorganization of ecological communities and ecosystem functions. As a key species for soil stabilization, its establishment in new northern and northwestern areas could enhance ecosystem resilience to erosion (Ding et al., 2009; Zhang, 2015). Meanwhile, its retreat from southern regions may create ecological vacancies, altering local biodiversity, species interactions, and ecosystem processes (Alexander et al., 2015; Felipe-Lucia et al., 2020). This dynamic exemplifies the complex cascade of climate-induced community reassembly, where the range shift of a single functionally important species can trigger broader changes in ecosystem properties (Zarnetske et al., 2012).

4.4. Biogeographic shifts and conservation implications under climate change

Our results provide strong support for our initial hypothesis that warming temperatures would drive a northward shift in the distribution of *H. acerba*. The consistent northwestward migration of the distribution centroid across all future climate scenarios (Fig. 9) directly aligns with this prediction. While the movement was predominantly northwestern rather than purely northern, this trajectory is logically explained by the topographical and climatic context of China. A due north trajectory from the current centroid in Hunan would encounter the mountainous regions of the Qinling-Daba Mountains, which may present topographic or ecological barriers that can significantly constrain species range shifts under climate change (Elsen and Tingley, 2015). The observed northwestward path, moving into Hubei and towards the Sichuan Basin, likely represents the species tracking its climatic niche along a path of least resistance into newly suitable areas. This nuanced finding not only confirms the general trend of poleward migration observed globally (Scheffers et al., 2016), but also refines our understanding of how regional geography modulates this global phenomenon.

The consistent northwestward migration of the distribution centroid under all climate scenarios provides robust evidence that *H. acerba* is tracking its climatic niche, thereby strongly supporting our initial hypothesis of a northward distributional shift (Chen et al., 2011; Pecl et al., 2017). The magnitude of centroid displacement, which increased with the intensity of greenhouse gas emissions, demonstrates a direct link between anthropogenic forcing and the velocity of range shifts (Diffenbaugh and Field, 2013; Loarie et al., 2009). Notably, the non-linear, southwestward trajectory under the extreme SSP5-8.5 scenario by the 2090s reveals that species responses to intense warming can deviate from simple poleward trends, likely due to complex interactions with topographic barriers and regional precipitation gradients (Elsen and Tingley, 2015; Lenoir and Svenning, 2015). This underscores that future species distributions will be shaped not only by macroclimatic trends but also by fine-scale heterogeneities in landscape and climate (Potter et al., 2013; Storlie et al., 2014).

These projected shifts present a dual conservation challenge: facilitating expansion into new suitable areas while securing vulnerable populations in contracting regions. The identified climate refugia, areas projected to remain suitable across scenarios, must be prioritized for protection as critical reservoirs for genetic diversity and population persistence (Keppel et al., 2012; Morelli et al., 2020). Conversely, proactive measures such as assisted migration and the establishment of ecological corridors are warranted to enhance connectivity and aid the species' natural colonization of future suitable habitats (Hoegh-Guldberg et al., 2008; Williams and Dumroese, 2013). Our

quantification of the distribution centroid's migration path offers a strategic guide for planning these corridors, effectively bridging the gap between climate impact science and actionable conservation management (Corlett and Westcott, 2013; Heller and Zavaleta, 2009; McGuire et al., 2016).

4.5. Management implications and adaptive strategies

Our spatially explicit projections for *H. acerba* provide a direct basis for developing climate-informed conservation strategies. We propose a tripartite approach, Protect, Connect, and Adapt, tailored to the species' projected distribution shifts: (1) Priority should be given to persistent suitable habitats in the southern core range (e.g., Chongqing, Guizhou, Hunan). These areas act as natural arks for genetic diversity and population persistence, requiring management that reduces non-climatic stressors like habitat fragmentation. (2) The northwestward centroid shift defines a strategic pathway for corridor planning and assisted migration. Introducing *H. acerba* into newly suitable areas of Hubei and southern Shaanxi, using climate-adapted seed sources, is especially critical under high-emission scenarios (SSP5-8.5). (3) In contracting areas, management should shift toward monitoring climate stress and facilitating ecological transition to more heat- and drought-tolerant species where *H. acerba* persistence becomes unlikely. This scenario-aware framework enables efficient resource allocation, helping stakeholders maintain *H. acerba* viability and its associated ecosystem services under changing climates.

5. Conclusions

Climate change is projected to reorganize the distribution of *Hovenia acerba* in China, triggering a northwestward range shift and a net expansion of suitable habitat. Our optimized MaxEnt model identified precipitation of the driest month (Bio14) and the minimum temperature of the coldest month (Bio6) as the dominant constraints on its distribution. The consistent northwestward migration of the distribution centroid—moving over 130 km from Hunan to Hubei under moderate emissions—confirms this trajectory. These findings translate into clear conservation priorities. The projected spatial shifts advocate for a dual management strategy: (1) designating climate refugia in the stable southern core range (e.g., Chongqing, Guizhou) for prioritized protection, and (2) implementing assisted migration and corridor establishment in the northwestern expansion zone (e.g., Hubei, S Shaanxi) to facilitate natural colonization. By aligning interventions such as targeted reforestation with these geographically explicit forecasts, our work provides a science-based blueprint for the adaptive management of *H. acerba*, ensuring the resilience of this ecologically and economically vital species under future climates.

CRediT authorship contribution statement

Yangzhou Xiang: Writing – original draft, Visualization, Validation, Investigation, Formal analysis, Data curation. **Suhang Li:** Writing – review & editing, Software, Data curation, Conceptualization. **Qiong Yang:** Writing – review & editing, Methodology, Data curation, Conceptualization. **Ying Liu:** Writing – review & editing, Software, Investigation, Conceptualization. **Jiaojiao Liu:** Writing – review & editing, Conceptualization. **Bin Yao:** Writing – review & editing, Supervision, Resources, Project administration, Conceptualization. **Yuan Li:** Writing – review & editing, Project administration, Investigation, Conceptualization.

Declaration of competing interest

The authors declare that they have no known competing financial interests or personal relationships that could have appeared to influence the work reported in this paper.

Acknowledgments

This work was supported by the Fundamental Research Funds for the Guizhou Provincial Science and Technology Projects (QKHJC-ZK [2022] YB335), and Guizhou Education University Scientific Research Fund Project (2024YB002; 2024BSKQ003).

Data availability

Data will be made available on request.

References

Alexander, J.M., Diez, J.M., Levine, J.M., 2015. Novel competitors shape species' responses to climate change. Nature 525 (7570), 515–518. https://doi.org/10.1038/nature14952.

Allen, C.D., Macalady, A.K., Chenchouni, H., Bachelet, D., McDowell, N., Vennetier, M., Kitzberger, T., Rigling, A., Breshears, D.D., Hogg, E.H., Gonzalez, P., Fensham, R., Zhang, Z., Castro, J., Demidova, N., Lim, J.-H., Allard, G., Running, S.W., Semerci, A., Cobb, N., 2010. A global overview of drought and heat-induced tree mortality reveals emerging climate change risks for forests. For. Ecol. Manag. 259 (4), 660–684. https://doi.org/10.1016/j.foreco.2009.09.001.

An, H., Zhao, Y., Ma, M., 2020. Precipitation controls seed bank size and its role in alpine meadow community regeneration with increasing altitude. Glob. Change Biol. 26 (10), 5767–5777. https://doi.org/10.1111/gcb.15260.

Brown, J.L., Bennett, J.R., French, C.M., 2017. SDMtoolbox 2.0: the next generation Python-based GIS toolkit for landscape genetic, biogeographic and species distribution model analyses. PeerJ 5, e4095. https://doi.org/10.7717/peerj.4095.

Chen, I.C., Hill, J.K., Ohlemüller, R., Roy, D.B., Thomas, C.D., 2011. Rapid range shifts of species associated with high levels of climate warming. Science 333 (6045), 1024–1026. https://doi.org/10.1126/science.1206432.

Cheng, R., Sun, M., Hu, Q., Deng, Z., Zhang, B., Li, H., 2023. *Hovenia acerba* Lindl. peduncles and seeds extracts ameliorate alcoholic liver injury by activating the Nrf2/HO-1 signalling pathway in LO2 cells and mice. Food Biosci. 51, 102224. https://doi.org/10.1016/j.fbio.2022.102224.

Choat, B., Jansen, S., Brodribb, T.J., Cochard, H., Delzon, S., Bhaskar, R., Bucci, S.J., Feild, T.S., Gleason, S.M., Hacke, U.G., Jacobsen, A.L., Lens, F., Maherali, H., Martínez-Vilalta, J., Mayr, S., Mencuccini, M., Mitchell, P.J., Nardini, A., Pittermann, J., Pratt, R.B., Sperry, J.S., Westoby, M., Wright, I.J., Zanne, A.E., 2012. Global convergence in the vulnerability of forests to drought. Nature 491 (7426), 752–755. https://doi.org/10.1038/nature11688.

Chuine, I., 2010. Why does phenology drive species distribution? Phil. Trans. Biol. Sci. 365 (1555), 3149–3160. https://doi.org/10.1098/rstb.2010.0142.

Corlett, R.T., Westcott, D.A., 2013. Will plant movements keep up with climate change? Trends Ecol. Evol. 28 (8), 482–488. https://doi.org/10.1016/j.tree.2013.04.003.

Diffenbaugh, N.S., Field, C.B., 2013. Changes in ecologically critical terrestrial climate conditions. Science 341 (6145), 486–492. https://doi.org/10.1126/science.1237123.

Ding, X., Ma, L., Chen, G., Du, D., 2009. The impact of soil moisture content on the growth and development of *Hovenia acerba*. Soil and Water Conservation in China (8), 51–52 (In Chinese with English Abstract).

Dolezal, J., Jandova, V., Macek, M., Mudrak, O., Altman, J., Schweingruber, F.H., Liancourt, P., 2021. Climate warming drives Himalayan alpine plant growth and recruitment dynamics. J. Ecol. 109 (1), 179–190. https://doi.org/10.1111/1365-2745.13459.

Elith, J., Graham, C.H., Anderson, R.P., Dudík, M., Ferrier, S., Guisan, A., Hijmans, R.J., Huettmann, F., Leathwick, J.R., Lehmann, A., Li, J.G., Lohmann, L., Loiselle, B.A., Manion, G., Moritz, C., Nakamura, M., Nakazawa, Y., McC, M., Overton, J., Townsend Peterson, A., Phillips, S.J., Richardson, K., Scachetti-Pereira, R., Schapire, R.E., Soberón, J., Williams, S., Wisz, M.S., Zimmermann, N.E., 2006. Novel methods improve prediction of species' distributions from occurrence data. Ecography 29 (2), 129–151. https://doi.org/10.1111/j.2006.0906-7590.04596.x.

Elith, J., Phillips, S.J., Hastie, T., Dudík, M., Chee, Y.E., Yates, C.J., 2011. A statistical explanation of MaxEnt for ecologists. Divers. Distrib. 17 (1), 43–57. https://doi.org/10.1111/j.1472-4642.2010.00725.x.

Elsen, P.R., Tingley, M.W., 2015. Global mountain topography and the fate of montane species under climate change. Nat. Clim. Change 5 (8), 772–776. https://doi.org/10.1038/nclimate2656.

Feeley, K.J., Bravo-Avila, C., Fadrique, B., Perez, T.M., Zuleta, D., 2020. Climate-driven changes in the composition of New World plant communities. Nat. Clim. Change 10 (10), 965–970. https://doi.org/10.1038/s41558-020-0873-2.

Felipe-Lucia, M.R., Soliveres, S., Penone, C., Fischer, M., Ammer, C., Boch, S., Boeddinghaus, R.S., Bonkowski, M., Buscot, F., Fiore-Donno, A.M., Frank, K., Goldmann, K., Gossner, M.M., Hölzel, N., Jochum, M., Kandeler, E., Klaus, V.H., Kleinebecker, T., Leimer, S., Manning, P., Oelmann, Y., Saiz, H., Schall, P., Schloter, M., Schöning, I., Schrumpf, M., Solly, E.F., Stempfhuber, B., Weisser, W.W., Wilcke, W., Wubet, T., Allan, E., 2020. Land-use intensity alters networks between biodiversity, ecosystem functions, and services. Proc. Natl. Acad. Sci. 117 (45), 28140–28149. https://doi.org/10.1073/pnas.2016210117.

Freeman, B.G., Lee-Yaw, J.A., Sunday, J.M., Hargreaves, A.L., 2018. Expanding, shifting and shrinking: the impact of global warming on species' elevational distributions. Global Ecol. Biogeogr. 27 (11), 1268–1276. https://doi.org/10.1111/geb.12774.

Ganjurjav, H., Gornish, E.S., Hu, G., Schwartz, M.W., Wan, Y., Li, Y., Gao, Q., 2020. Warming and precipitation addition interact to affect plant spring phenology in alpine meadows on the central Qinghai-Tibetan Plateau. Agric. For. Meteorol. 287, 107943. https://doi.org/10.1016/j.agrformet.2020.107943.

Gong, X., Chen, Y., Wang, T., Jiang, X., Hu, X., Feng, J., 2020. Double-edged effects of climate change on plant invasions: ecological niche modeling global distributions of two invasive alien plants. Sci. Total Environ. 740, 139933. https://doi.org/10.1016/j.scitotenv.2020.139933.

Heller, N.E., Zavaleta, E.S., 2009. Biodiversity management in the face of climate change: a review of 22 years of recommendations. Biol. Conserv. 142 (1), 14–32. https://doi.org/10.1016/j.biocon.2008.10.006.

Hoegh-Guldberg, O., Hughes, L., McIntyre, S., Lindenmayer, D.B., Parmesan, C., Possingham, H.P., Thomas, C.D., 2008. Assisted colonization and rapid climate change. Science 321 (5887), 345–346. https://doi.org/10.1126/science.1157897.

Huan, Z., Geng, X., Xu, X., Liu, W., Zhu, Z., Tang, M., 2023. Potential geographical distribution of *Michelia martinii* under different climate change scenarios based on MaxEnt model. J. Ecol. Rural Environ. 39 (10), 1277–1287 (In Chinese with English Abstract).

Keppel, G., Van Niel, K.P., Wardell-Johnson, G.W., Yates, C.J., Byrne, M., Mucina, L., Schut, A.G.T., Hopper, S.D., Franklin, S.E., 2012. Refugia: identifying and understanding safe havens for biodiversity under climate change. Global Ecol. Biogeogr. 21 (4), 393–404. https://doi.org/10.1111/j.1466-8238.2011.00686.x.

Khan, A.M., Li, Q., Saqib, Z., Khan, N., Habib, T., Khalid, N., Majeed, M., Tariq, A., 2022. MaxEnt modelling and impact of climate change on habitat suitability variations of economically important chilgoza pine (*Pinus gerardiana* Wall.) in south Asia. Forests 13 (5). https://doi.org/10.3390/f13050715.

Kong, Y., Yan, H., Wang, C., Shi, C., Tian, B., 2023. Studies on the hypoglycemic activity and substance basis of *Hovenia acerba lindl* pulp and seed in vitro and in vivo. J. Chin. Inst. Food Sci. Technol. 23 (12), 87–96 (In Chinese with English Abstract).

Lenoir, J., Svenning, J.C., 2015. Climate-related range shifts – a global multidimensional synthesis and new research directions. Ecography 38 (1), 15–28. https://doi.org/10.1111/ecog.00967.

Li, Y., Li, M., Li, C., Liu, Z., 2020. Optimized Maxent model predictions of climate change impacts on the suitable distribution of *Cunninghamia lanceolata* in China. Forests 11 (3), 302. https://doi.org/10.3390/f11030302.

Lindborg, R., Ermold, M., Kuglerová, L., Jansson, R., Larson, K.W., Milbau, A., Cousins, S. A.O., 2021. How does a wetland plant respond to increasing temperature along a latitudinal gradient? Ecol. Evol. 11 (22), 16228–16238. https://doi.org/10.1002/ece3.8303.

Loarie, S.R., Duffy, P.B., Hamilton, H., Asner, G.P., Field, C.B., Ackerly, D.D., 2009. The velocity of climate change. Nature 462 (7276), 1052–1055. https://doi.org/10.1038/nature08649.

Lü, Z., Zhu, X., Ye, X., Wen, G., Jiang, T., Lai, W., Shi, C., Huang, Q., Zhang, G., 2024. Impacts of climate change on the suitable habitats and spatial migration of *Tetraena mongolica*. Acta Ecol. Sin. 44 (3), 1164–1176 (In Chinese with English Abstract).

Ma, X., Zhou, H., 2022. *Hovenia acerba* Lindl.: an insight into botany, phytochemistry, bioactivity, quality control, and exploitation. J. Food Biochem. 46 (12), e14434. https://doi.org/10.1111/jfbc.14434.

MacDougall, A.S., Caplat, P., Olofsson, J., Siewert, M.B., Bonner, C., Esch, E., Lessard-Therrien, M., Rosenzweig, H., Schäfer, A.-K., Raker, P., Ridha, H., Bolmgren, K., Fries, T.C.E., Larson, K., 2021. Comparison of the distribution and phenology of Arctic Mountain plants between the early 20th and 21st centuries. Glob. Change Biol. 27 (20), 5070–5083. https://doi.org/10.1111/gcb.15767.

Mantyka-Pringle, C.S., Visconti, P., Di Marco, M., Martin, T.G., Rondinini, C., Rhodes, J. R., 2015. Climate change modifies risk of global biodiversity loss due to land-cover change. Biol. Conserv. 187, 103–111. https://doi.org/10.1016/j.biocon.2015.04.016.

McGuire, J.L., Lawler, J.J., McRae, B.H., Nuñez, T.A., Theobald, D.M., 2016. Achieving climate connectivity in a fragmented landscape. Proc. Natl. Acad. Sci. 113 (26), 7195–7200. https://doi.org/10.1073/pnas.1602817113.

Mendes, P., Velazco, S.J.E., Andrade, A.F.A.d., De Marco, P., 2020. Dealing with overprediction in species distribution models: how adding distance constraints can improve model accuracy. Ecol. Model. 431, 109180. https://doi.org/10.1016/j.ecolmodel.2020.109180.

Morelli, T.L., Barrows, C.W., Ramirez, A.R., Cartwright, J.M., Ackerly, D.D., Eaves, T.D., Ebersole, J.L., Krawchuk, M.A., Letcher, B.H., Mahalovich, M.F., Meigs, G.W., Michalak, J.L., Millar, C.I., Quiñones, R.M., Stralberg, D., Thorne, J.H., 2020. Climate-change refugia: biodiversity in the slow Lane. Front. Ecol. Environ. 18 (5), 228–234. https://doi.org/10.1002/fee.2189.

Muscarella, R., Galante, P.J., Soley-Guardia, M., Boria, R.A., Kass, J.M., Uriarte, M., Anderson, R.P., 2014. ENMeval: an R package for conducting spatially independent evaluations and estimating optimal model complexity for Maxent ecological niche models. Methods Ecol. Evol. 5 (11), 1198–1205. https://doi.org/10.1111/2041-210X.12261.

Numata, S., Yamaguchi, K., Shimizu, M., Sakurai, G., Morimoto, A., Alias, N., Noor Azman, N.Z., Hosaka, T., Satake, A., 2022. Impacts of climate change on reproductive phenology in tropical rainforests of Southeast Asia. Commun. Biol. 5 (1), 311. https://doi.org/10.1038/s42003-022-03245-8.

Pearson, R.G., Dawson, T.P., 2003. Predicting the impacts of climate change on the distribution of species: are bioclimate envelope models useful? Global Ecol. Biogeogr. 12 (5), 361–371. https://doi.org/10.1046/j.1466-822X.2003.00042.x.

Pecl, G.T., Araújo, M.B., Bell, J.D., Blanchard, J., Bonebrake, T.C., Chen, I.C., Clark, T.D., Colwell, R.K., Danielsen, F., Evengård, B., Falconi, L., Ferrier, S., Frusher, S., Garcia, R.A., Griffis, R.B., Hobday, A.J., Janion-Scheepers, C., Jarzyna, M.A., Jennings, S., Lenoir, J., Linnetved, H.I., Martin, V.Y., McCormack, P.C., McDonald, J., Mitchell, N.J., Mustonen, T., Pandolfi, J.M., Pettorelli, N., Popova, E., Robinson, S.A., Scheffers, B.R., Shaw, J.D., Sorte, C.J.B., Strugnell, J.M., Sunday, J. M., Tuanmu, M.-N., Vergés, A., Villanueva, C., Wernberg, T., Wapstra, E., Williams, S.E., 2017. Biodiversity redistribution under climate change: impacts on ecosystems and human well-being. Science 355 (6332), eaai9214. https://doi.org/10.1126/science.aai9214.

Peng, H., Deng, Z., Chen, X., Sun, Y., Zhang, B., Li, H., 2018. Major chemical constituents and antioxidant activities of different extracts from the peduncles of *Hovenia acerba* Lindl. Int. J. Food Prop. 21 (1), 2135–2155. https://doi.org/10.1080/10942912.2018.1497059.

Phillips, Steven J., Dudík, Miroslav, Schapire, Robert E.. [Internet] Maxent software for modeling species niches and distributions (version 3.4.1). Available from: url: http://biodiversityinformatics.amnh.org/open_source/maxent/. (Accessed 16 July 2024).

Potter, K.A., Arthur Woods, H., Pincebourde, S., 2013. Microclimatic challenges in global change biology. Glob. Change Biol. 19 (10), 2932–2939. https://doi.org/10.1111/gcb.12257.

Qian, D., 2022. Maxent Model Analysis on the Evolution of Woody Plant Distribution Pattern in the Amur River Basin Under Climate Change. Northeast Forestry University, Haerbin.

Scheffers, B.R., De Meester, L., Bridge, T.C.L., Hoffmann, A.A., Pandolfi, J.M., Corlett, R. T., Butchart, S.H.M., Pearce-Kelly, P., Kovacs, K.M., Dudgeon, D., Pacifici, M., Rondinini, C., Foden, W.B., Martin, T.G., Mora, C., Bickford, D., Watson, J.E.M., 2016. The broad footprint of climate change from genes to biomes to people. Science 354 (6313). https://doi.org/10.1126/science.aaf7671 aaf7671.

Shi, J., Xia, M., He, G., Gonzalez, N.C.T., Zhou, S., Lan, K., Ouyang, L., Shen, X., Jiang, X., Cao, F., Li, H., 2024. Predicting *Quercus gilva* distribution dynamics and its response to climate change induced by GHGs emission through MaxEnt modeling. J. Environ. Manag. 357, 120841. https://doi.org/10.1016/j.jenvman.2024.120841.

Storlie, C., Merino-Viteri, A., Phillips, B., VanDerWal, J., Welbergen, J., Williams, S., 2014. Stepping inside the niche: microclimate data are critical for accurate assessment of species' vulnerability to climate change. Biol. Lett. 10 (9), 20140576. https://doi.org/10.1098/rsbl.2014.0576.

Teng, J., Zhou, Z., 2016. Research on *Hovenia acerba* community characteristics in Macheng City. Hubei ForestryScience and Technology 45 (2), 9–12 (In Chinese with English Abstract).

Wang, M., Guan, Q., 2023. Prediction of potential suitable areas for Broussonetia papyrifera in China using the MaxEnt model and CIMP6 data. J. Plant Ecol. 16 (4), 1–16. https://doi.org/10.1093/jpe/rtad006.

Wang, Z., Wang, T., Zhang, X., Wang, J., Yang, Y., Sun, Y., Guo, X., Wu, Q., Nepovimova, E., Watson, A.E., Kuca, K., 2024. Biodiversity conservation in the context of climate change: facing challenges and management strategies. Sci. Total Environ. 937, 173377. https://doi.org/10.1016/j.scitotenv.2024.173377.

Warren, D.L., Seifert, S.N., 2011. Ecological niche modeling in Maxent: the importance of model complexity and the performance of model selection criteria. Ecol. Appl. 21 (2), 335–342. https://doi.org/10.1890/10-1171.1.

Williams, M.I., Dumroese, R.K., 2013. Preparing for climate change: forestry and assisted migration. J. For. 111 (4), 287–297. https://doi.org/10.5849/jof.13-016.

Williams, S.E., Shoo, L.P., Isaac, J.L., Hoffmann, A.A., Langham, G., 2008. Towards an integrated framework for assessing the vulnerability of species to climate change. PLoS Biol. 6 (12), e325. https://doi.org/10.1371/journal.pbio.0060325.

Yang, Z., Chen, H., Lin, C., Sun, J., Wen, W., Zhu, X., El-Kassaby, Y.A., Feng, J., 2023. Comprehensive evaluation of quality traits of *Hovenia acerba* germplasm resources in Fujian Province. Forests 14 (2). https://doi.org/10.3390/f14020204.

Ye, X., Zhao, G., Zhang, M., Cui, X., Fan, H., Liu, B., 2020. Distribution pattern of endangered plant *Semiliquidambar cathayensis* (Hamamelidaceae) in response to climate change after the last interglacial period. Forests 11 (4). https://doi.org/10.3390/f11040434.

Yu, G., Yin, H., Wang, G., Chen, R., 2008. Study on the seed selection of raisin tree seed and digest time in Chinese ferret-badger. Chin. J. Ecol. 25 (3), 51–53 (In Chinese with English Abstract).

Yu, A., Yang, Y., Yang, Y., Liang, M., Zheng, F., Sun, B., 2020. Free and bound aroma compounds of turnjujube (*Hovenia acerba* Lindl.) during low temperature storage. Foods 9 (4). https://doi.org/10.3390/foods9040488.

Zarnetske, P.L., Skelly, D.K., Urban, M.C., 2012. Biotic multipliers of climate change. Science 336 (6088), 1516–1518. https://doi.org/10.1126/science.1222732.

Zhang, J., 2015. Research on the cultivation effects of local tree species *Hovenia acerba*. Forestry Survey and Design (Fujian) (1), 153–156 (In Chinese with English Abstract).

Zhang, K., Yao, L., Meng, J., Tao, J., 2018. Maxent modeling for predicting the potential geographical distribution of two peony species under climate change. Sci. Total Environ. 634, 1326–1334. https://doi.org/10.1016/j.scitotenv.2018.04.112.

Zhang, Y., Liu, Y., Qin, H., Meng, Q., 2019. Prediction on spatial migration of suitable distribution of *Elaeagnus mollis* under climate change conditions in Shanxi Province, China. Chin. J. Appl. Ecol. 30 (2), 496–502 (In Chinese with English Abstract).

Zhang, M., Ye, X., Liu, Y., Li, J., Chen, S., Zhang, G., Liu, B., 2022. Predicting the potential geographical distribution of *Erythrophleum fordii* in China based on SSPs. J. Beijing For. Univ. 44 (4), 54–65 (In Chinese with English Abstract).

Zhang, X., Zhang, L., Zhang, Y., Xiong, T., Niu, Y., Huang, Y., 2023. Extracting myricetin and dihydromyricetin simultaneously from Hovenia acerba seed by Ultrasound-Assisted extraction on a lab and small Pilot-Scale. Ultrason. Sonochem. 93, 106304. https://doi.org/10.1016/j.ultsonch.2023.106304.

Zhang, X., Nizamani, M.M., Jiang, C., Fang, F., Zhao, K., 2024. Potential planting regions of Pterocarpus santalinus (Fabaceae) under current and future climate in China based on MaxEnt modeling. Ecol. Evol. 14 (6), e11409. https://doi.org/10.1002/ece3.11409.

Zhao, Z., Xiao, N., Shen, M., Li, J., 2022. Comparison between optimized MaxEnt and random forest modeling in predicting potential distribution: a case study with

Quasipaa boulengeri in China. Sci. Total Environ. 842, 156867. https://doi.org/10.1016/j.scitotenv.2022.156867.

Zhao, J., Shao, W., Li, Y., Chen, H., Lin, Z., Wei, L., 2024. Potential impact of climate change on the distribution of Capricornis milneedwardsii, a vulnerable mammal in China. Ecol. Evol. 14 (6), e11582. https://doi.org/10.1002/ece3.11582.

Zhou, T., Chen, Z., Zou, L., Chen, X., Yu, Y., Wang, B., Bao, Q., Bao, Y., Cao, J., He, B., Hu, S., Li, L., Li, J., Lin, Y., Ma, L., Qiao, F., Rong, X., Song, Z., Tang, Y., Wu, B., Wu, T., Xin, X., Zhang, H., Zhang, M., 2020. Development of climate and Earth System models in China: past achievements and new CMIP6 results. J. Meteorol. Res. 34 (1), 1–19. https://doi.org/10.1007/s13351-020-9164-0.

Zhu, K., Woodall, C.W., Clark, J.S., 2012. Failure to migrate: lack of tree range expansion in response to climate change. Glob. Change Biol. 18 (3), 1042–1052. https://doi.org/10.1111/j.1365-2486.2011.02571.x.